

## SPECTRAL FEATURES OF E- AND F-REGION PLASMA IRREGULARITIES AS OBSERVED BY ROCKET-BORNE ELECTRON DENSITY PROBES FROM BRAZIL

Polinaya Muralikrishna<sup>1</sup>, Leandro Paulino Vieira<sup>2</sup> and Mangalathayil Ali Abdu<sup>3</sup>

Recebido em 12 dezembro, 2005 / Aceito em 5 outubro, 2006  
Received on December 12, 2005 / Accepted on October 5, 2006

**ABSTRACT.** The height variation of the ionospheric electron density was measured with rocket-borne electron density probes from Alcântara (2.31°S; 35.2°W) in Brazil. A Black Brant X sounding rocket was launched on 14-th October 1994 at 19h55min (LT) to investigate the phenomenon of high-altitude equatorial spread-F events. Ground equipments were operated during the campaign to ensure that the rocket was launched under conditions favorable for the generation of plasma bubbles in the F-region. The electron density was measured by three different types of probes. A High Frequency Capacitance probe (HFC) gave density data with low height resolution, while a conventional Langmuir Probe (LP) and a Plasma Frequency Probe (PFP) measured the electron density and the spatial fluctuations in it. The  $k$ -spectra of the plasma irregularities were obtained by the spectral analysis of the electron density fluctuation data. An important feature observed was the continuous presence of plasma irregularities of a large range of vertical scale sizes in the altitude range of 340 km to 817 km. The electron number density varied considerably in these spatial structures, for example a decrease by a factor of 2.6 in a vertical extension of 1 km near the altitude of 497 km. Near 535 km altitude the electron density increased by a factor of 1.8 within a height range of 2.7 km. Density structures of vertical scale sizes in the range of hundreds of meters also were observed superposed on the large-scale structures. During the rocket upleg two height regions of intense irregularities were observed, one between 366 and 480 km and the other between 684 and 812 km. The Langmuir Probe (LP) could make measurements of irregularities of vertical scale sizes more than 8 m in these height ranges, while the Plasma Frequency Probe, could make measurements of irregularities of vertical scale sizes as small as 0.5 m. Spectral features of these irregularities as observed by the two plasma probes at different height regions are presented and discussed here.

**Keywords:** ionosphere, space plasma, plasma irregularities, rocket measurements, plasma density probes.

**RESUMO.** A variação com altura da densidade eletrônica na ionosfera foi medida com sondas de densidade eletrônica a bordo de foguetes de Alcântara (2.31°S; 35.2°O) no Brasil. Um foguete de sondagem "Black Brant X" foi lançado no dia 14 de outubro de 1994 às 19h55min (LT) para investigar o fenômeno de Espalhamento-F na alta ionosfera equatorial. Equipamentos foram operados na superfície terrestre durante a campanha para assegurar que o foguete foi lançado nas condições favoráveis pela geração das bolhas de plasma na região-F. A densidade eletrônica foi medida por três tipos diferentes de sondas. Uma sonda capacitiva em alta frequência (HFC) forneceu os dados de densidade eletrônica de baixa resolução, quando uma sonda de Langmuir (LP) convencional e uma sonda de frequência de plasma (PFP) mediram a densidade e as flutuações espaciais nela. Os espectros-k das irregularidades de plasma foram obtidas pela análise espectral dos dados de flutuações de densidade eletrônica. Uma característica importante observada foi a presença contínua das irregularidades de plasma de uma faixa larga de escalas de tamanho vertical na faixa de altura de 340 km a 817 km. A densidade numérica de elétrons variou consideravelmente nestas estruturas espaciais, por exemplo uma diminuição por um fator de 2,6 numa extensão vertical de 1 km perto da altura de 497 km. Perto da altura de 535 km a densidade aumentou por um fator de 1,8 numa faixa de altura de 2,7 km. Estruturas de densidade de escalas verticais na faixa de centenas de metros também foram observadas superpostas nas escalas largas. Durante a subida do foguete duas faixas de altura das irregularidades intensas foram observadas, uma entre 366 e 480 km e a outra entre 684 e 812 km. A sonda de Langmuir (LP) fez medidas das irregularidades da escala vertical maior que 8 m nestas faixas de altura, quando a sonda de frequência de plasma (PFP) fez medidas das irregularidades da escala vertical de até 0,5 m. As características especiais destas irregularidades como observadas pelas duas sondas de plasma nas regiões de diferentes alturas são apresentadas e discutidas aqui.

**Palavras-chave:** ionosfera, plasma espacial, irregularidades de plasma, medidas com foguetes, densidade de plasma, sondas de densidade de plasma.

<sup>1</sup>National Institute for Space Research, INPE, P.O. Box 515 – 12201-970 São José dos Campos, SP, Brazil. Phone: +55 (12) 3045-7148; Fax: +55 (12) 3945-6990 – E-mail: murali@dae.inpe.br

<sup>2</sup>Aeronomy Division, DAE, National Institute for Space Research, INPE, P.O. Box 515 – 12201-970 São José dos Campos, SP, Brazil.

<sup>3</sup>National Institute for Space Research, INPE, P.O. Box 515 – 12201-970 São José dos Campos, SP, Brazil. Phone: +55 (12) 3045-7149; Fax: +55 (12) 3945-6990 – E-mail: maabdu@dae.inpe.br

## INTRODUCTION

Electron density irregularities present in the ionosphere manifest themselves in different forms at different heights and times. Sporadic-E, spread-F, radio star scintillations and VHF radar echoes are a few of such phenomena, familiar to ionospheric physicists. Basic knowledge of the plasma irregularities, responsible for these phenomena, has progressed considerably, both in theory and observations, since the discovery of the strong VHF radar echoes from the equatorial ionosphere (Bowles et al., 1960, 1963). Balsley (1969), from their spectral characteristics as observed by the VHF radar, classified the plasma irregularities into two groups, namely Type I and Type II. While the Type I irregularities are now identified to be consistent with the two-stream instability mechanism (Farley, 1963; Sato, 1972), the Type II irregularities are known to be produced by the nonlinear cross-field instability mechanism (Rogister & d'Angelo, 1970, 1972; Balsley & Farley, 1973). Direct observations by Prakash et al. (1970, 1971a,b) using rocket-borne Langmuir probes flown from India, confirm the existence of the Type II irregularities in the equatorial E-region. Type II irregularities are characterized by scale sizes extending from a few meters up to tens of kilometres. The short wavelength irregularities apparently seem to be generated from larger scale sizes by nonlinear coupling or cascading processes (Rogister, 1972; Rogister & d'Angelo, 1970, 1972; Sato 1971, 1973; Sudan et al., 1973). Neutral turbulence also seems to be another probable mechanism responsible for the generation of plasma irregularities (Prakash et al., 1970). The spectral characteristics of the different types of irregularities have been studied in detail (Prakash et al., 1970; Ott & Farley, 1974).

Plasma bubbles, flux tubes of depleted plasma density, observed frequently in the equatorial night time ionosphere have been the subject of active investigation in the last couple of decades (see Abdu et al., 1991 and references therein). These bubbles are characterised by scale lengths of thousands of kilometres along the geomagnetic field lines and tens to hundreds of kilometres perpendicular to the field lines. Their generation through the Rayleigh-Taylor (R-T) gravitational instability process and subsequent cascading, by secondary processes, into a hierarchy of irregularities was suggested by Haerendel (1974).

Some new results obtained from in-situ measurements of the height variation of the ionospheric electron density made with rocket-borne electron density probes during a rocket campaign conducted from Alcântara (2.31°S; 35.2°W) in Brazil are presented here.

## EXPERIMENT AND FLIGHT DETAILS

### Guará campaign

During the Guará campaign conducted from Alcântara, Brazil, a Black Brant X rocket was launched on 14-th October, 1994 at 19h55min (LT) with the main objective of studying the equatorial ionosphere during the presence of high altitude plasma bubbles. The electron density height profile and the amplitude of the electron density fluctuations were measured simultaneously by the following three plasma density probes:

- A High Frequency Capacitance (HFC) probe
- A conventional Langmuir Probe (LP)
- A Plasma Frequency Probe (PFP)

### High Frequency Capacitance probe

Neglecting collision and magnetic field effects, one can get a simple relationship between the ambient electron density and the oscillator frequency of a HFC probe (Heikkila et al., 1968) as:

$$n = \frac{2 \cdot f^2 \cdot \Delta f (C_s + C_0)}{81 \cdot f_0 \cdot S \cdot C_0} \quad (1)$$

where,  $n$  is the number density of electrons,  $f$  is the oscillator frequency in the plasma,  $f_0$  is the oscillator frequency in free space,  $\Delta f$  is the variation in the oscillator frequency,  $C_0$  is the capacitance of the sensor in free space,  $C_s$  is the stray capacitance of the oscillator,  $S$  is the plasma sheath factor.

The variation in the oscillator frequency for a given ambient plasma density is inversely proportional to the oscillator frequency (Eq. 1). Lower the oscillator frequency higher is the sensitivity of measurement. But the equation 1 is valid only when the oscillator frequency is well above the local ionospheric plasma frequency that can vary by orders of magnitude from the lower E-region to the upper F-region and also between outside and inside the plasma bubbles. To cover the large dynamic range of the electron density and also to study the relative behavior of the ion sheath, the HFC experiment operated in two modes alternately with frequencies of about 5 MHz and 10 MHz. The duration of operation in each mode was about 60 ms, thus giving a data point in each mode every 120 ms. To obtain the free space oscillator frequency negative bias pulses of 100V is applied to the HFC sensor for a short time (128 ms in the present case) at regular intervals of time. This repels the ambient plasma from the neighborhood of the sensor and the oscillator frequency measured during this period is very close to the free space oscillator frequency. Changes (up to about 10% from the mean value) in the frequency of

oscillation is measured and later converted into the ambient electron number density within the measurable range of  $10^3$  to  $5 \times 10^6$  electrons per cubic centimeter.

In the present case, the HFC Probe used a spherical sensor of 52 mm diameter mounted on a short boom deployed 108 s after the launch of the rocket. The High Frequency Capacitance probe was designed and developed in the laboratories of the Aeronomy Division of the National Institute for Space Research-INPE/MCT.

### Langmuir Probe

A conventional Langmuir Probe, operating in the saturation ion current mode was launched on board the rocket to measure the ion number density, which is the same as the electron number density in a quasi-neutral ionospheric plasma. When operating in the saturation electron or ion current mode the electron (ion) number density is proportional to the measured current and can be easily estimated by normalizing with some absolute measurement of the electron density like that from a Plasma Frequency Probe or from a ground based Digisonde. It is now well established that the electron number density estimated from the measured saturation ion current is more reliable than that estimated from the saturation electron current (Brace, 1998). Electron number density estimated from the electron saturation current collected by a probe is seen to be approximately 20 percent more than that estimated from the ion saturation current, and sometimes an empirically derived normalization factor is applied to the electron density based on the ratio of the electron density to ion density measured in regions of higher density where the ion density can be measured accurately (Brace, 1998). However, the accuracy of electron density measurements made by a conventional LP is limited by several factors like, the plasma sheath effect, the effect of the vehicle floating potential, contamination of the probe surface, secondary electron and photo emission from the sensor surface etc (see Muralikrishna & Abdu, 1991).

The Langmuir Probe data presented here are provided by the Department of Physics and Astronomy, Dartmouth College, USA.

### Plasma Frequency Probe

In a Plasma Frequency Probe (PFP) a signal with swept frequency is transmitted using a short antenna on board the rocket at fixed short intervals of time and the signal that traverses through the ambient plasma and thereby gets modified by the plasma is received using another short antenna on board. When the signal frequency becomes equal to the ambient plasma frequency the signal

amplitude falls down drastically due to the resonant absorption by the ambient plasma. What is monitored in this experiment is the height variation in the plasma frequency that is decided by the ambient plasma density. A PFP can provide absolute electron number densities. The antenna exhibits a resonance at the upper hybrid frequency of the magnetoplasma,  $f_H$  defined by,

$$f_H^2 = f_N^2 + f_B^2 \quad (2)$$

where

$$f_B = \frac{eB}{2\pi m_e}$$

is the electron gyro frequency, and

$$f_N^2 = \frac{e^2 N}{4\pi^2 \epsilon_0 m_e}$$

is the electron plasma frequency.

In the above equations,  $e$  is the electronic charge,  $B$  is the ambient geomagnetic field flux,  $m_e$  is the electronic mass,  $N$  is the electron number density, and  $\epsilon_0$  is the free space dielectric constant. By using the appropriate value of the terrestrial magnetic field, one can estimate the electron plasma frequency from the measured upper hybrid frequency, and thereby calculate the electron density.

The Plasma Frequency Probe data presented here are provided by the Department of Physics and Astronomy, Dartmouth College, USA.

## RESULTS

### Electron density profiles

Electron density height profiles obtained during the Guara campaign from the analysis of the HFC, LP and PFP data during the upleg and downleg of the rocket are shown in Figures 1 and 2 respectively. To facilitate comparison of each profile with the other they shifted along the  $x$ -axis as indicated by the three scales along the axis in both the figures. The scale for the PFP profile is indicated along the bottom left half of the  $x$ -axis, that for the HFC on the top, and that for the LP along the bottom right half of the  $x$ -axis. The upleg profiles at altitudes below about 300 km are contaminated by interference signal from the attitude control system of the rocket and are not shown in Figure 1. A successful attempt was made to remove this systematic signal from the LP data, and therefore the LP profile is available at the E-region altitudes also. The fluctuation data corresponding to the electron density variations could be separated from the interference signal and therefore

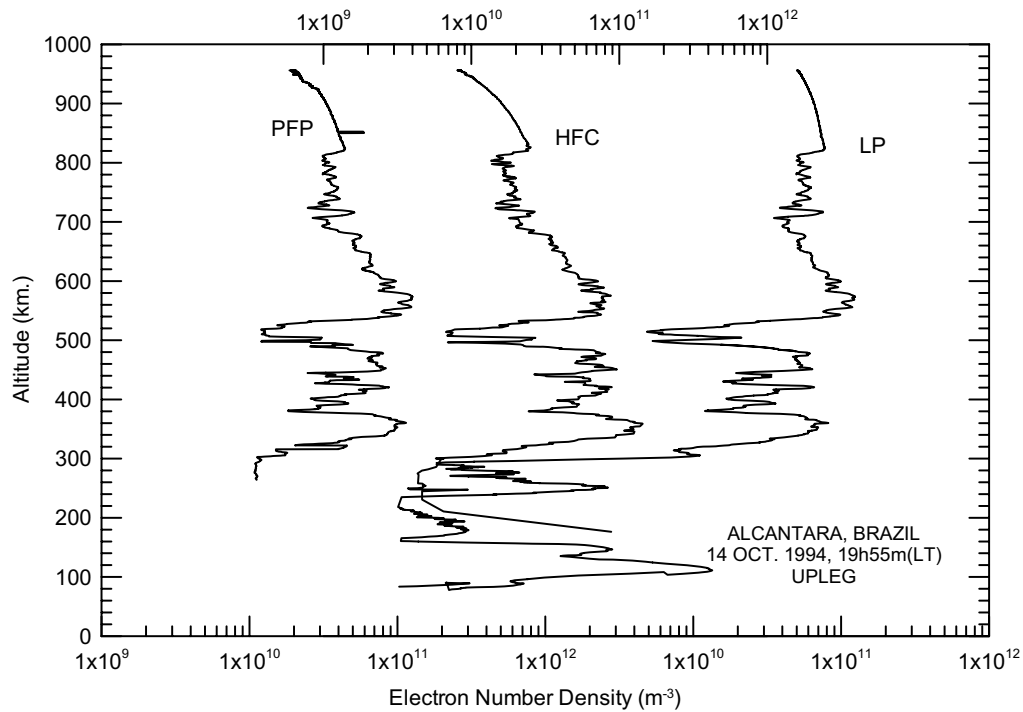


**Figure 1** – Upleg electron density profiles obtained from a Plasma Frequency Probe (PFP – bottom left scale), a High Frequency Capacitance probe (HFC – top center scale) and a Langmuir Probe (LP – bottom right scale) during the campaign Guar.

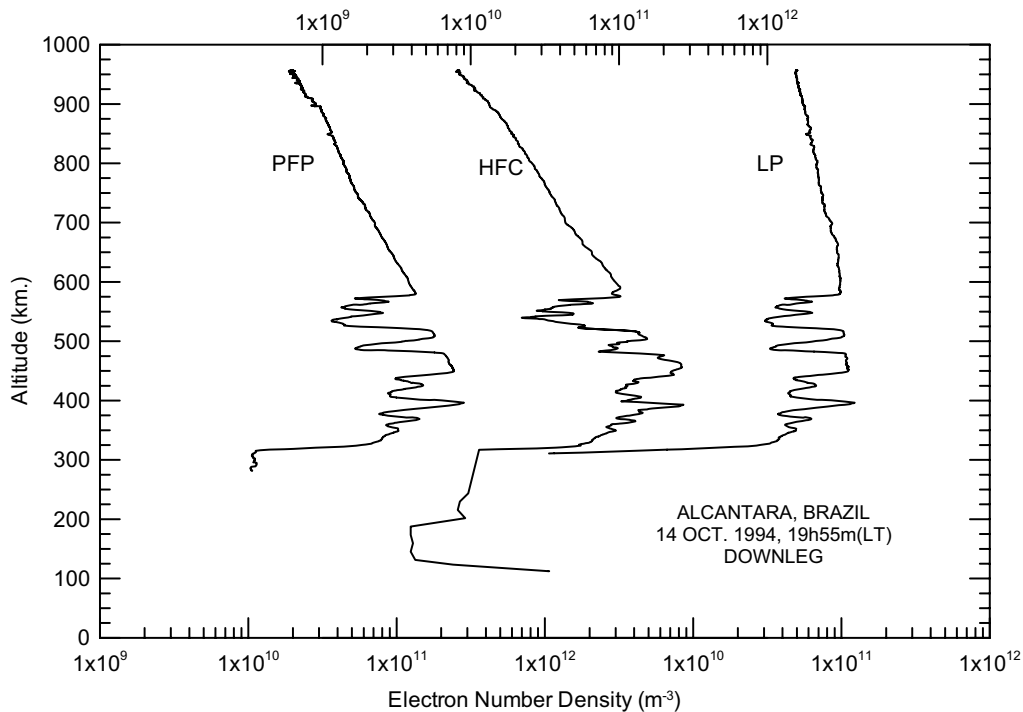


**Figure 2** – Downleg electron density profiles obtained from a Plasma Frequency Probe (PFP – bottom left scale), a High Frequency Capacitance probe (HFC – top center scale) and a Langmuir Probe (LP – bottom right scale) during the campaign Guar.

the spectral data provided for the E-region altitudes for both PFP and LP signals are reliable.

The plasma density profiles estimated from the three experiments agree reasonably well with each other, especially when one considers the general profile and the large-scale variations in it. A close look at the electron density height profiles clearly shows the existence of a wide spectrum of scale sizes in the plasma irregularities. All the upleg height profiles clearly show the presence of irregularities associated with what is known as the phenomenon of high altitude Spread-F. The presence of medium amplitude plasma bubbles in the high altitude region can be seen in all the upleg profiles while the profiles from the LP and PFP experiments give an idea of the distribution of the small-scale irregularities in this height region. An important feature observed in all the profiles is the continuous presence of plasma irregularities of a large range of vertical scale sizes in the altitude range of 340 km to 817 km. Plasma bubbles with dimensions of a few kilometres to several tens of kilometres along the rocket trajectory are observed in the height region of 350 km to 550 km during the upleg of the rocket. The electron number density varied considerably in these spatial structures, for example a decrease by a factor of 2.6 in a vertical extension of 1 km near the altitude of 497 km. Near 535 km altitude the electron density increased by a factor of 1.8 within a height range of 2.7 km. Density structures of vertical scale sizes in the range of hundreds of meters also were observed superposed on the large-scale structures. During the rocket upleg two height regions of intense irregularities were observed, one between 366 and 480 km and the other between 684 and 812 km. The LP and PFP experiments have sufficient height resolution to study the amplitude fluctuations in the small-scale plasma irregularities down to a few meters, while the HFC experiment has a height resolution with typical values of about 100 m near the altitude of 300 km. The Langmuir Probe (LP) could make measurements of irregularities of vertical scale sizes more than 8 m in these height ranges, while the Plasma Frequency Probe, could make measurements of irregularities of vertical scale sizes as small as 0.5 m. For all the three experiments the height resolution improves with height due to the decrease in the rocket velocity.

The rocket downleg profiles shown in Figure 2 clearly show the presence of a wide spectrum of irregularities in the height region of 300–600 km, but not in the high altitude region. This probably is due to the limited horizontal extent of the high altitude Spread-F event responsible for the generation of plasma irregularities. The horizontal separation of the upleg and downleg trajectory of the rocket in this height region can vary from few tens of

km to about 200 km. This distance, therefore, roughly represents the east-west horizontal extension of the high altitude plasma bubbles or the phenomenon of high altitude Spread-F associated with these bubbles. Detailed spectral analysis of the density data at different height regions was done to know the spectral distribution of these plasma irregularities and thereby to know the plasma instability mechanisms responsible for their generation.

### ***k*-spectra of irregularities**

Typical *k*-spectra obtained from the spectral analysis of the electron density fluctuation data of the HFC, LP and PFP experiments are shown in Figures 3 to 8. A striking feature of the spectra, shown on a linear scale in the Figures 3 to 5 is the presence of spectral peaks of large amplitudes in practically all the *k*-spectra, a hitherto unobserved feature. Figure 3 shows the *k*-spectra of large-scale irregularities estimated from the HFC probe density data for a few selected height regions during the rocket upleg. The relative spectral power (*y*-axis) is plotted against the wave number *k* of the irregularities (*x*-axis). Unlike the conventional *k*-spectra which are shown on a log-log scale, the spectra in the present case are on linear scales along the *x* and *y* axes. The lower most curve in Figure 3, represents the spectral amplitude observed in the height region of 323 to 367 km, which is the base of the F-region. The presence of at least two dominant peaks corresponding to wave numbers of  $0.0002 \text{ m}^{-1}$  (wavelength  $\lambda \cong 31 \text{ km}$ ) and  $0.0008 \text{ m}^{-1}$  ( $\lambda \cong 7.8 \text{ km}$ ) can be seen in the spectrum. At higher altitudes, though there are indications of spectral peaks, they are not dominant. The power spectra obtained from the LP and PFP density data at a few selected heights are shown in Figures 4 and 5. It should be noted here that the wave number *k* of the irregularities shown along the *x*-axis extends approximately from 0 to  $1 \text{ m}^{-1}$ . In Figure 3 where the spectra obtained are from the HFC density data, the *k* value ranges from 0 to  $0.001 \text{ m}^{-1}$ , while the corresponding range of *k* in Figure 4 representing the LP density data ranges from  $0.001 \text{ m}^{-1}$  to  $0.05 \text{ m}^{-1}$  and in Figure 4 from  $0.05 \text{ m}^{-1}$  to  $1 \text{ m}^{-1}$ . Figures 3, 4 and 5 thus confirm the presence of sharp spectral peaks in the entire wave number regime, though with varying powers at different altitudes.

### **Spectral index**

Typical *k*-spectra of plasma irregularities obtained from the LP density measurements, for selected heights extending from 117 km in the E-region to 710 km in the F-region are shown in Figures 6 and 7. The spectral power along the *y*-axis is plotted against the wave number *k* of the irregularities along the *x*-

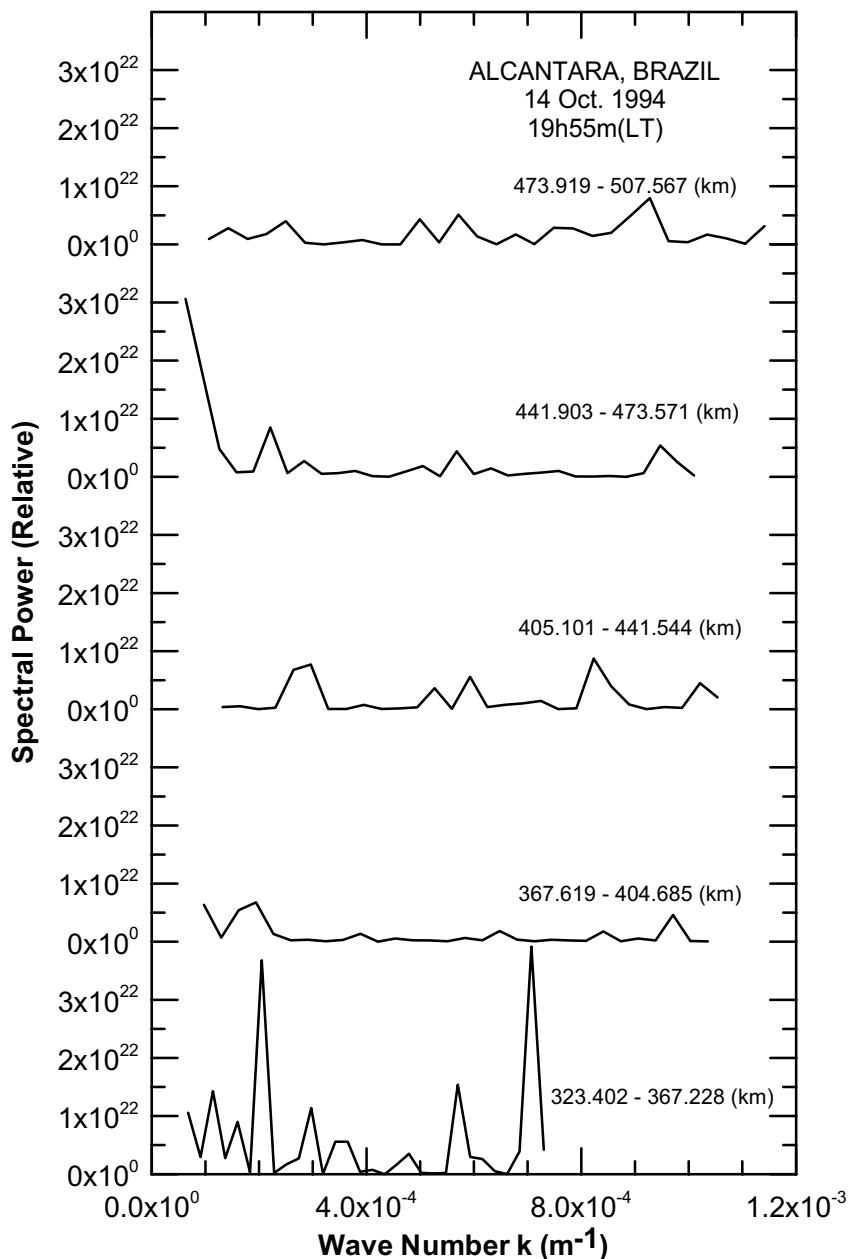


**Figure 3** – Typical nature of the  $k$ -spectra of plasma irregularities, obtained from the HFC probe measurements showing the presence of sharp peaks.

axis is plotted in the conventional way on a log-log scale. Corresponding spectra estimated for the PFP electron density data are shown in Figure 8 for selected F- region heights, for the purpose of comparison with the LP spectra shown in Figures 6 and 7. Unlike in the linear plots shown in Figures 3 to 5, the sharp spectral peaks cannot be dominantly seen in the log-log presentation. The spectral index  $n$  that dictates the power law dependence of

the spectral power  $P(k)$  on the wave number  $k$  through the relation  $P(k) \propto k^n$  is estimated for each spectrum and is also indicated in the Figures 6 to 8. The mean height corresponding to the spectrum is shown along with each spectrum. Practically all the spectra show two distinct parts with different values for the spectral index  $n$ , one corresponding to the lower  $k$  values (larger scale sizes) and another to higher  $k$  values (smaller scale sizes).

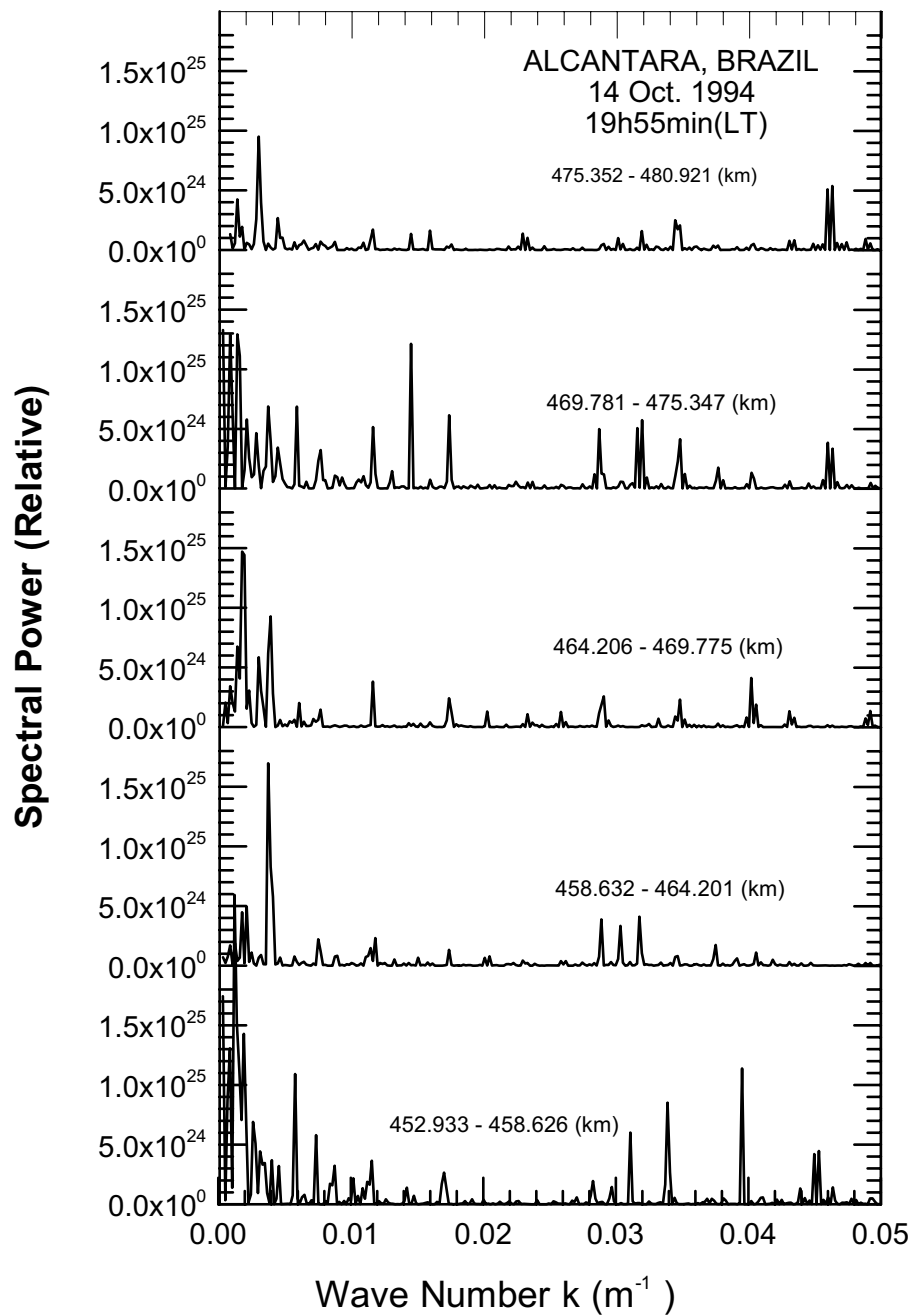


**Figure 4** – Typical nature of the  $k$ -spectra of plasma irregularities, obtained from the Langmuir probe (LP) measurements showing the presence of sharp peaks.

In both the E- and F- regions the spectra observed have similar features characteristic of irregularities generated by the mechanism of Cross-Field Instability (CFI). The spectra estimated for the F- region heights from the LP and PFP electron density data also have very similar characteristic features and spectral indices in the same range of values for the different range of  $k$  values.

## DISCUSSION

Observation of bubble structures in the night time ionosphere is rather a familiar feature. It is now a rather well established fact that the plasma bubbles are characterized by scale lengths of thousands of kilometres along the geomagnetic field lines and tens of

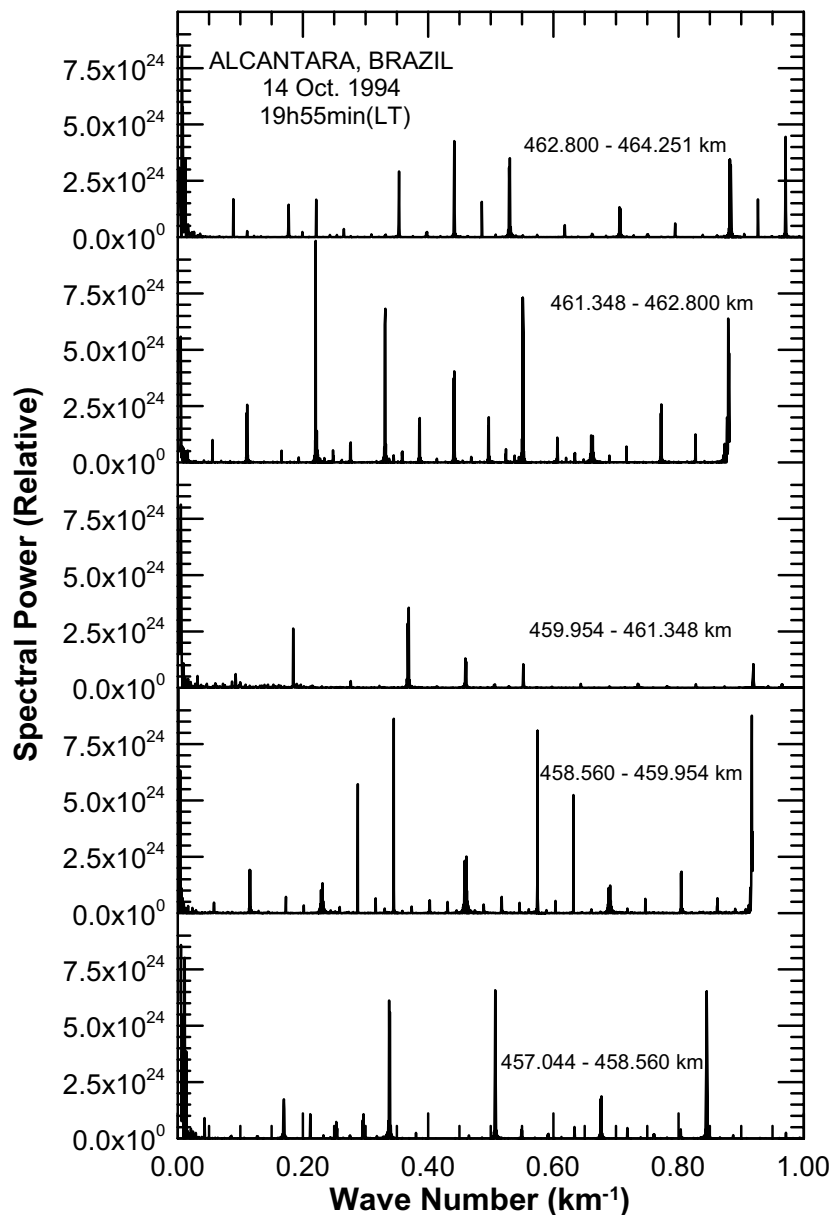


**Figure 5** – Typical nature of the  $k$ -spectra of plasma irregularities, obtained from the Plasma Frequency Probe (PFP) probe measurements showing the presence of sharp peaks.

hundreds of kilometres perpendicular to the field lines. Their generation through the Rayleigh-Taylor (R-T) gravitational instability process and subsequent cascading, by secondary processes, into a hierarchy of irregularities was suggested by Haerendel (1974). The spectral characteristics of the different types of irregularities associated with the phenomenon of spread-F have been studied in detail (Prakash et al., 1970; Ott & Farley, 1974). The generation of small-scale plasma irregularities by the mechanism of cross-field

instability (CFI) is also now reasonably well understood (Reid, 1968; Tsuda et al., 1969). A necessary condition for the mechanism to operate in the E-region altitudes (Gradient Drift Instability – GDI) is that there should exist an electron density gradient in the direction of the ambient electric field. The GDI mechanism is a variant of the Rayleigh-Taylor Instability (RTI) mechanism and is excited when the equilibrium density gradient and the ambient electric field are in the same direction (Hu & Bhattacharjee, 1999).



## LP – UPLEG SPECTRA

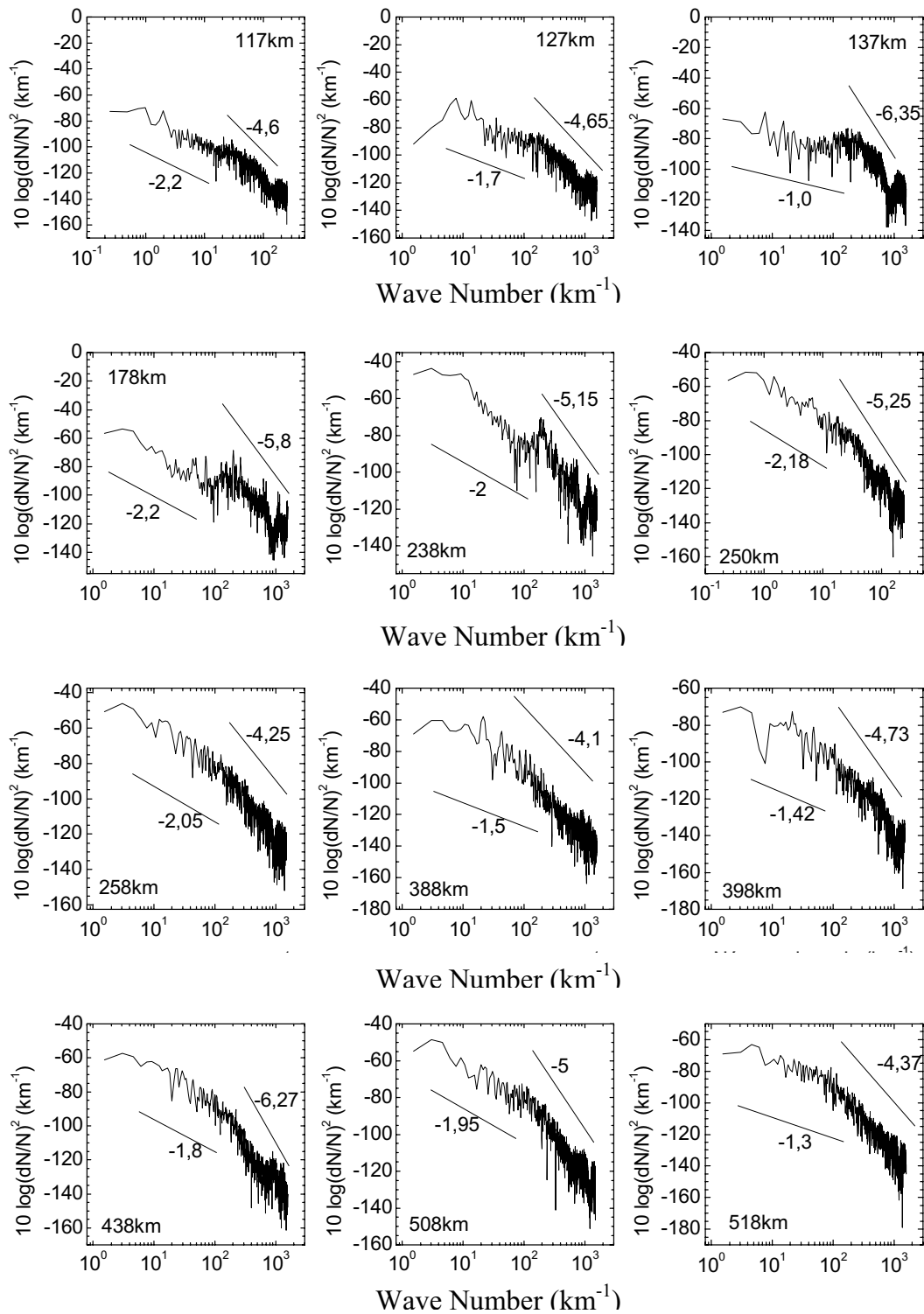


**Figure 6** – Typical nature of the  $k$ -spectra of plasma irregularities, obtained from the Langmuir probe (LP) measurements showing the spectral indices.

## LP – UPLEG SPECTRA (Contd.)

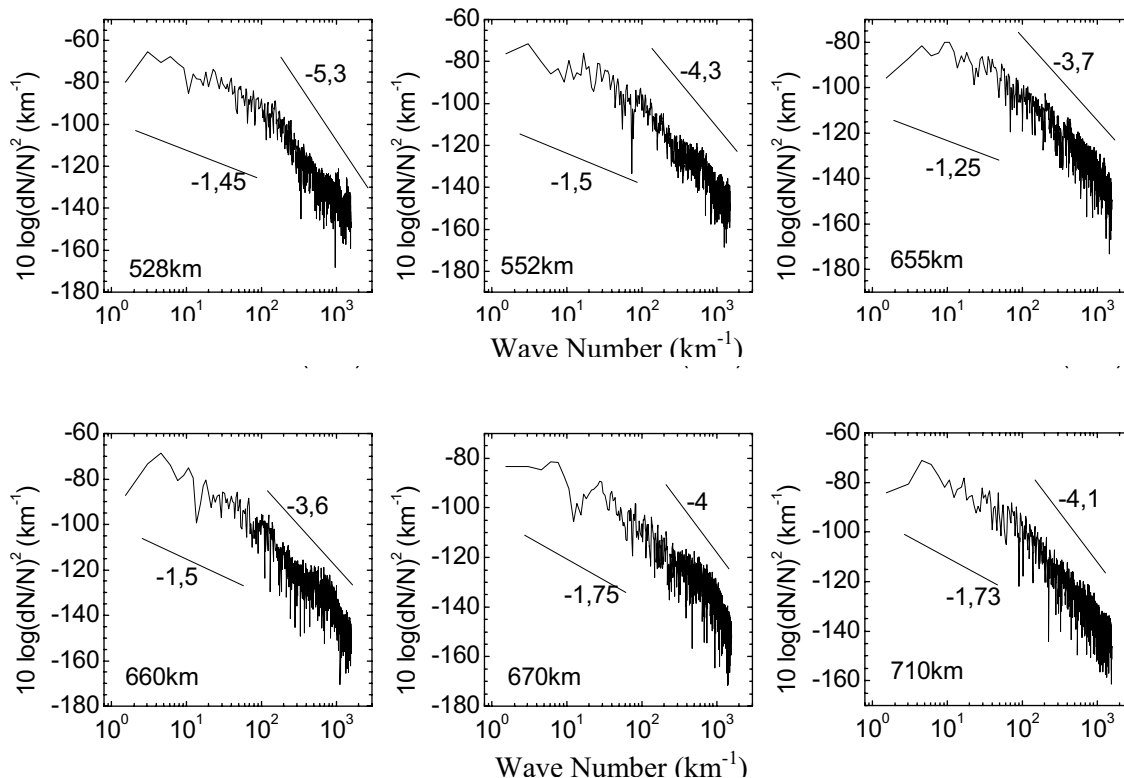


Figure 7 – Typical nature of the  $k$ -spectra of plasma irregularities, obtained from the Langmuir probe (LP) measurements showing the spectral indices.

In the F-region altitudes the CFI mechanism (**ExB** Instability – EBI mechanism) can operate at regions where the zonal component of the ambient electric field is westward (eastward) and the electron density gradient is downward (upward). In the night time ionosphere the primary electric field is generally westward and the Hall polarisation field is generally downward. So the height regions favourable for the operation of CFI mechanism are those where the ambient electron density gradients are also downwards. However the presence of plasma irregularities in the bottom side F-region where the E-field is supposed to be downwards and the electron density gradient is upwards cannot be attributed to the operation of the CFI mechanism. But small-scale plasma irregularities can be generated in the region of downward electron density gradients associated with the large-scale bubbles seen in this height region.

The small-scale irregularities produced by the CFI mechanism are expected to have a rather flat  $k$ -spectrum as the earlier observations showed and as predicted by the existing theories on the generation of plasma irregularities. A striking new feature ob-

served during the experiments reported here is the presence of large spectral peaks in the  $k$ -spectra of the plasma irregularities. One should note here that the rocket flight reported here was conducted during the onset period of the ionospheric plasma bubbles and therefore represent the characteristic features of plasma irregularities associated with new or developing plasma bubbles. One can explain such sharp spectral lines if one assumes that there exist preferred modes for the growth of an instability mechanism, something similar to the existence of natural frequencies in a mechanical vibration or oscillation. These modes are the first ones to be excited during the growth of an instability process. It is possible that as time progresses the plasma irregularities responsible for these spectral peaks, transfer their energy to lower and lower scale size irregularities and thus eventually lead to a flat  $k$ -spectrum when the process attains the equilibrium or stable state. But a theory that can explain these spectral peaks even during the development phase of the plasma bubbles is not known yet.

The electron density irregularities are known to exhibit their

PFP – UPLEG SPECTRA

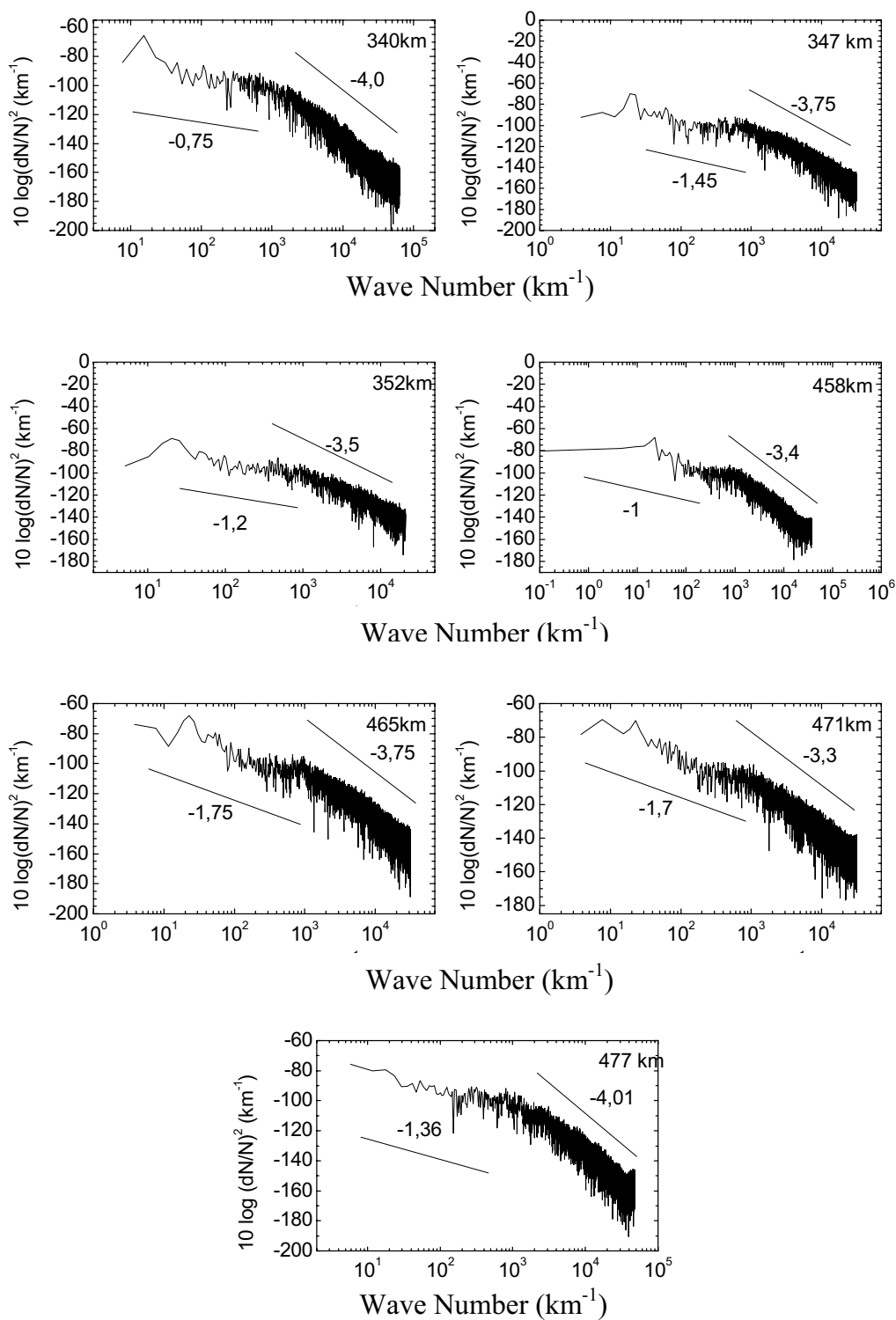


Figure 8 – Typical nature of the  $k$ -spectra of plasma irregularities, obtained from the Plasma Frequency Probe (PFP) probe measurements showing the spectral indices.

characteristic spectral distribution depending on the altitude range of their generation and the plasma instability mechanism responsible for it. Larger scale size irregularities generated by the RTI mechanism exhibit a lower spectral index  $n$  (a flatter spectrum) while the smaller scale size irregularities generated by the CFI mechanism exhibit a steeper spectrum with  $n$  reaching values between  $-4.5$  and  $-5.0$ .

Kelley et al. (1976) presented the first evidence that plasma bubbles generated at the bottom side F-region through the RTI mechanism can rise due to buoyancy forces and can attain altitudes far above the region unstable to the RTI mechanism. This partly can explain the high altitude spread-F in terms of the primary instability operating below the peak in F-region electron density. For the same flight Costa & Kelley (1978) found a power law of the type  $k^n$  with spectral index  $n = -2.0$  for the steep coherent density structures of scale size (scale size  $\lambda = 2\pi/k$  where  $k$  is the wave number) in the range between 10 km and 10 m ( $k$  in the range between  $0.628 \text{ km}^{-1}$  and  $628 \text{ km}^{-1}$ ) in the bottom side F-region.

Rino et al. (1981) found that for electron density irregularities with scale sizes between 5 km and 500 m ( $k$  between  $1.257 \text{ km}^{-1}$  and  $12.57 \text{ km}^{-1}$ ) the spectral index  $n$  ranged between  $-1.2$  and  $-2.5$  and for irregularities with scale sizes between 50 m and 500 m ( $k$  between  $125.7 \text{ km}^{-1}$  and  $12.57 \text{ km}^{-1}$ ) the  $n$  value was between  $-2.3$  and  $-3.4$  indicating steeper spectra for altitudes below 370 km. For higher altitudes the observed  $n$  values ranged between  $-1.2$  and  $-2.6$ . The break in spectrum was observed around 500 m ( $k = 12.57 \text{ km}^{-1}$ ). Such a break in the spectrum is also noticed in spectra presented in Figures 6 to 8 where irregularity spectral powers are plotted against the wave number  $k$  of irregularities for different height regions and also as observed by different electron density probes.

Keskinen et al. (1981) discussed one dimensional bottom side irregularity spectra exhibiting a spectral index of  $-2.5$  for scale sizes in the range of 1 km to tens of meters and developed a computational mode of RTI that supported the experimental results. Kelley et al. (1982) from Plumex electron density data reported a  $n$  value of  $-2.0$  for long wavelengths and  $n$  values between  $-4.5$  and  $-5.0$  for scale sizes less than 100 m, for altitudes above 280 km. LaBelle et al. (1986) also reported from rocket experiments conducted in Punta Lobos, Peru, for altitudes above 280 km, spectral indices of  $n = -2.0$  for scale sizes greater than 100 m and  $n = -4.5$  for scale sizes less than 100 m. Hysell et al. (1994) reported from Kwajalein rocket observations, spectral indices of  $-2.0$  and  $-4.5$  for scale sizes above and below about 100 m ( $k$  values below and above  $62.83 \text{ km}^{-1}$ ) respectively.

The spectral indices estimated for the irregularity spectra reported here and shown in Figures 6 to 8 are in very good agreement with the earlier observations, namely less than  $-2.0$  for the larger scale size irregularities and close to  $-4.5$  for the smaller scale size irregularities. An important point to be noted here is the fact that the spectra presented in Figures 3, to 5 and where the power axis is on a linear scale are the same as those presented in Figures 6 to 8 where the power axis is on a log scale. The good agreement between the earlier observations of the spectral index and those reported here, all the more consolidates the importance of the observation of large spectral peaks in the linear power spectra.

## CONCLUSIONS

1. Electron Density height profiles estimated from different types of experiments namely a High Frequency capacitance probe, a Langmuir probe and a Plasma Frequency Probe during the occurrence of the phenomenon of High Altitude Spread-F agree well with each other.
2. Plasma irregularities of a wide spectrum of scale sizes are dominantly seen at E-region (F-region) heights where the electron density gradients are downwards and the Hall polarisation field (the primary electric field) is downward (westward), confirming their association with the well known cross-field instability mechanism for the generation of plasma irregularities.
3. The generation of large scale plasma structures in the bottom side of the F-region cannot be explained by the cross-field instability mechanism that needs the vertical electric field and the electron density gradient to be in the same direction.
4. Bubble regions are associated with a wide spectrum of plasma irregularities or electron density fluctuations. Spectral analysis of the AC data clearly show the presence of large peaks in the  $k$ -spectra of the plasma irregularities
5. The existing theories for the generation of plasma irregularities cannot explain the sharp spectral peaks observed in the  $k$ -spectra.
6. One possible explanation for the presence of large peaks in the  $k$ -spectrum of irregularities is that they may be associated only with developing plasma bubbles and may dissipate their energy with time thus leading to a flat  $k$ -spectrum as the steady state is reached.

7. The spectral indices estimated from the present data for the different altitudes are in good agreement with those reported from earlier observations.

### ACKNOWLEDGEMENTS

The authors are grateful to the Directors of IAE/CTA and CLA, Alcântara for providing the rockets and the launch facilities respectively and to the staff of IAE and CLA for their help during the pre-launch tests of the experiments, and during the launching of the rockets. Sincere thanks are to Sinval Domingos, Agnaldo Eras and Narli Baesso Lisboa for their technical help in the development testing and integration of the experiments. The work reported here was partially supported by FINEP under contract FINEP-537/CT, and by CNPq under process 300253/89-3/GM/FV.

### REFERENCES

- ABDU M, MURALIKRISHNA P, BATISTA IS & SOBRAL JHA. 1991. Rocket observation of equatorial plasma bubbles over Natal, Brazil using a High Frequency Capacitance probe. *J. Geophys. Res.*, 96: 7689–7695.
- BALSLEY BB. 1969. Some characteristics of non-two-stream irregularities in the equatorial electrojet. *J. Geophys. Res.*, 74: 2333–2347.
- BALSLEY BB & FARLEY DT. 1973. Radar observation of two-dimensional turbulence in the equatorial electrojet. *J. Geophys. Res.*, 78: 7471–7479.
- BRACE LH. 1998. Langmuir Probe measurements in the ionosphere. In: PFAFF RF, BOROVSKY JE & YOUNG DT (Ed.). *Measurement Techniques in Space Plasmas*. American Geophysical Union, Washington, DC, 23–35.
- BOWLES KL, COHEN R, OCHS AR & BALSLEY BB. 1960. Radar echoes from field aligned ionisation above the magnetic equator and their resemblance to auroral echoes. *J. Geophys. Res.*, 65: 1853–1855.
- BOWLES KL, BALSLEY BB & COHEN R. 1963. Field aligned E-region irregularities identified with acoustic plasma waves. *J. Geophys. Res.*, 68: 2485–2501.
- COSTA E & KELLEY MC. 1978. On the role of steepened structures and drift waves in equatorial spread-F. *J. Geophys. Res.*, 83: 4359–4364.
- FARLEY DT. 1963. Two stream instability as a source of irregularities in the ionospheres. *Phys. Rev. Lett.*, 10: 279–282.
- HAERENDEL G. 1974. Theory of equatorial spread-F, Report of Max Planck Institut für Physik und Astrophysik, Garching, Germany.
- HEIKKILA WJ, BAKER N, FEJER JA, TIPPLE KR, HUGILL J, SCEINBLE DE & CALVERT W. 1968. Comparison of several techniques for ionospheric electron density measurements. *J. Geophys. Res.*, 73: 3511.
- HU S & BHATTACHARJEE A. 1999. Gradient drift instabilities in the night time equatorial electrojet. *J. Geophys. Res.*, 104: 28123.
- HYSELL DL, KELLEY MC, SWARTZ WE, PFAFF RF & SWENSON CM. 1994. Steepened structures in equatorial spread-F: 1. New observations. *J. Geophys. Res.*, 99(A5): 8827–8840.
- KELLEY MC, HAERENDEL G, KAPPLER H, VALENZUELA A, BALSLEY BB, CARTER DA, ECKLUND WL, CARLSON CW, HAUSLER B & TORBERT R. 1976. Evidence for a Rayleigh-Taylor type instability and upwelling of depleted density regions during equatorial spread-F. *Geophys. Res. Lett.*, 3: 448–450.
- KELLEY MC, LIVINGSTON RC, RINO CL & TSUNODA RT. 1982. The vertical wave number spectrum of topside equatorial spread-F: Estimates of backscatter levels and implications for a unified theory. *J. Geophys. Res.*, 87: 5217.
- KESKINEN MJ, SZUSZCZEWICZ EP, OSSAKOW SL & HOLMES JC. 1981. Nonlinear theory and experimental observations of the local collisional Rayleigh-Taylor instability in a descending equatorial spread-F ionosphere. *J. Geophys. Res.*, 86: 5785–5792.
- LABELLE J, KELLEY MC & SEYLER CE. 1986. An analysis of the role of drift waves in equatorial spread-F. *J. Geophys. Res.*, 91: 5513–5525.
- MURALIKRISHNA P & ABDU MA. 1991. In situ measurement of ionospheric electron density by two different techniques – a comparison. *J. Atmos. Terr. Phys.*, 53: 787–793.
- OTT E & FARLEY DT. 1974. The  $k$  spectrum of ionospheric irregularities. *J. Geophys. Res.*, 79: 2469–2472.
- PRAKASH S, GUPTA SP & SUBBARAYA BH. 1970. A study of irregularities in the night time equatorial E-region using a Langmuir probe and a plasma noise probe. *Planet. Space Sci.*, 18: 1307–1318.
- PRAKASH S, GUPTA SP & SUBBARAYA BH. 1971a. Cross-field instability and ionisation irregularities in equatorial E-region. *Nature Phys. Sci.*, 230: 170.
- PRAKASH S, GUPTA SP, SUBBARAYA BH & JAIN CL. 1971b. Electrostatic plasma instabilities in the equatorial electrojet. *Nature Phys. Sci.*, 233: 56.
- REID GC. 1968. Small-scale irregularities in the ionosphere. *J. Geophys. Res.*, 73: 1627–1640.
- RINO CL, TSUNODA RT, PETRICEKS J, LIVINGSTON RC, KELLEY MC & BAKER KD. 1981. Simultaneous rocket-borne beacon and in situ measurements of equatorial spread-F. *J. Geophys. Res.*, 86: 2411.
- ROGISTER A. 1972. Nonlinear theory of cross-field instability with application to the equatorial electrojet. *J. Geophys. Res.*, 77: 2975–2981.
- ROGISTER A & D'ANGELO N. 1970. Type II irregularities in the equatorial electrojet. *J. Geophys. Res.*, 75: 3879–3887.
- ROGISTER A & D'ANGELO N. 1972. On the origin of small-scale Type II irregularities in the equatorial electrojet. *J. Geophys. Res.*, 77: 6298–6299.

SATO T. 1971. Nonlinear theory of the cross-field instability – explosive mode coupling. *Phys. Fluids*, 14: 2426–2435.

SATO T. 1972. Stabilization of the two-stream instability in the equatorial electrojet. *Phys. Rev. Lett.*, 28: 732–734.

SATO T. 1973. A unified theory of Type I and II irregularities in the equatorial electrojet. *J. Geophys. Res.*, 78: 2232–2243.

SUDAN RN, AKINRIMISI J & FARLEY DT. 1973. Generation of small-scale irregularities in the equatorial electrojet. *J. Geophys. Res.*, 78: 240–248.

TSUDA T, SATO T & MATSUSHITA S. 1969. Ionospheric irregularities and cross-field plasma instability. *J. Geophys. Res.*, 74: 2923–2932.

## NOTES ABOUT THE AUTHORS

**Polinaya Muralikrishna.** Graduated in Physics and Mathematics, in 1967, at the University of Kerala, India. He obtained his Master's Degree in Physics, in 1969, at the University of Kerala, and Doctor's Degree in Equatorial Aeronomy, in 1975, at the Physical Research Laboratory, University of Gujarat, India. Presently he is working as a Senior Scientist in the Aeronomy Division of the Instituto Nacional de Pesquisas Espaciais – INPE/MCT. His areas of interest are Aeronomy, Space Geophysics and Rocket and Satellite-borne Instrumentation.

**Leandro Paulino Vieira.** Graduated in Industrial Mechanical Engineering, in 1998, at Escola de Engenharia Industrial de São José dos Campos-SP, Brazil. He did the Course of Technician/Professional, in 1992, at the Departamento Regional de São Paulo, SENA/SP, Brazil and Master's Degree in Space Geophysics, in 2002, at the Instituto Nacional de Pesquisas Espaciais – INPE/MCT, Brazil. His areas of interest are Industrial Mechanical Engineering and Space Geophysics.

**Mangalathayil Ali Abdu.** Graduated in Physics, in 1959, at the Maharaja's College, University of Kerala, India. He obtained his Master's Degree, in 1961, at the Maharaja's College, University of Kerala, India and Doctor's Degree in Ionospheric Physics, in 1966, at the Physical Research Laboratory, University of Gujarat, India. Presently he is working as a Senior Scientist in the Aeronomy Division of the Instituto Nacional de Pesquisas Espaciais – INPE/MCT. His areas of interest are Aeronomy, Space Geophysics and Rocket and Satellite-borne Instrumentation.